On the role of the length of GPS time-series in the accuracy of tectonic velocities' estimation: Examples from the HEPOS network

Michail Gianniou[1], Eleni Mitropoulou[2], Dimitrios Mastoris[3]

[1] Hellenic Cadastre - 288 Messogion Ave., 155 62 Athens, Greece, (mgianniu@ktimatologio.gr)
[2] Hellenic Cadastre - 288 Messogion Ave., 155 62 Athens, Greece, (emitropo@ktimatologio.gr)
[3] Hellenic Cadastre - 288 Messogion Ave., 155 62 Athens, Greece, (dmastori@ktimatologio.gr)

Key words: *permanent reference stations; GPS time-series; tectonic velocities; Precise-point-positioning; HEPOS*

ABSTRACT

Permanent GPS reference stations are used since many years worldwide for a variety of purposes ranging from positioning services to realization of reference frames and scientific research. Permanent reference stations provide an excellent opportunity to estimate reliable tectonic velocities. Especially in cases that a reference station remains at its initial site for a long time-period, highly accurate velocities can be estimated. Today, there are many examples of stations that are operating on the same point for longer than 10 or even 20 years. These stations offer a good possibility to study the role of the length of GPS time-series in the accuracy of the estimation of tectonic velocities. In this work, we use data from the Hellenic Positioning System (HEPOS) to investigate the relationship between the length of the time-series and the accuracy of the resulting velocities. GPS observations from selected HEPOS stations are processed using the Precise-Point-Positioning (PPP) technique to obtain daily solutions. The velocities of each station are estimated multiple times using variable data length andthe results are compared to each other in order to reveal the impact of the length of the time-series to the accuracy of the estimated velocities. The analysis indicates that a minimum of 3 years of data should be used for velocity estimation and that 4 or more years can lead to horizontal velocity estimations accurate to a few tenths of mm/yr. We also investigate the role of the sampling rate of the GPS time-series in the accuracy of the results. The results are discussed in conjunction with the different reference frames of the PPP solutions and the noise characteristics of each time-series.

I. INTRODUCTION

The knowledge of accurate coordinates and velocities for the permanent reference stations is necessary for the operation of national RTK networks. In the case of the Hellenic Positioning System (HEPOS), the necessity to monitor the stations' coordinates becomes crucial, as Greece is the seismo-tectonically most active area in Europe (Hollenstein, 2006). In the framework of operating HEPOS, tectonic velocities of the stations are estimated taking into consideration discontinuities induced by geological phenomena like earthquakes and volcanic activity (Gianniou and Stavropoulou, 2016).

Traditionally, station velocities are estimated from coordinates obtained from a least squares adjustment of baseline vectors (carrier-phase relative positioning) that form a geodetic network. An alternative for estimating velocities is by means of coordinates computed using the Precise-Point-Positioning (PPP) technique (Zumberge *et al*., 1997). Calais *et al*. (2006) compared velocities obtained using relative positioning and PPP and found the results to agree to each other within 0.6-0.8 mm/yr on average for the horizontal velocity component and within 3 mm/yr for the vertical component. More recent research using latest software developments are reporting even better agreement between velocities obtained from PPP and relative positioning. For example, Walpersdorf *et al*. (2017) found an agreement between the two velocity solutions in the order of 0.12 mm/yr and 0.37 mm/yr for the horizontal and the vertical component, respectively.

Regardless of the method used for the processing of the GPS raw data, two questions arise in the process of estimating stations' velocities: First, how many years of observations are required to ensure reliable velocity estimation? Second, how critical is the sampling interval to the accuracy of estimated velocities? This paper investigates these aspects for the case of time-series of daily solutions obtained using the Precise-Point-Positioning technique.

II. PRECISE POINT POSITIONING

Precise Point Positioning uses dual frequency stand-alone observations to deliver cm-level precision. This technique requires precise satellite ephemerides and satellite clock parameters as well as careful modeling of many effects that in relative positioning cancel-out (Kouba and Héroux, 2001).

A. *Mathematical model*

The simplified observation equations for PPP are:

$$l_p = \rho + c(dt - dT) + Tr + \varepsilon_p \quad (1)$$
$$l_\phi = \rho + c(dt - dT) + Tr + N\lambda + \varepsilon_\phi \quad (2)$$

where l_p is the iono-free code observable
l_ϕ is the iono-free carrier phase observable
ρis the geometric distance satellite-receiver
dt is the receiver clock offset
dT is the satellite clock offset
c is the vacuum speed of light
Tr is the tropospheric delay
λis the iono-free wavelength
N is the iono-free phase ambiguity
$\varepsilon_p$is the code measurement noise
$\varepsilon_\phi$is the phase measurement noise

Other effects that do not appear in the simplified equations (1) and (2) and should be considered include: satellite antenna offset, antenna phase center variations, phase wind-up, solid earth tides, ocean loading and earth rotation parameters.

B. *Reference frames*

In PPP processing no fiducial points are used and the reference frame of the obtained coordinates is defined solely by the reference frame in which the precise orbits are expressed. Within the time span of the analyzed GPS data, the reference frame of the IGS products was changed three times. As a consequence, the obtained PPP results are expressed in four different frames: IGS05, IGS08, IGb08 and IGS14. Table 1 gives the beginning and the end of using each frame.

Table 1. IGS reference frames

Frame	In use	
	From	To
IGS05	5 Nov. 2006	16 Apr. 2011
IGS08	17 Apr. 2011	6 Oct. 2012
IGb08	7 Oct. 2012	28 Jan. 2017
IGS14	29 Jan. 2017	present

Although models for transforming between successive IGS frames are published, the application of those models in the practice should be considered carefully. Apart from a 14-parameter global transformation due to the underlying successive ITRF frames, additional coordinates shifts should be applied to account for the different antenna calibration models used for the realization of each frame. For example, ITRF2005 was based on relative antenna calibrations, while IGS05 used absolute calibrations (Schmid *et al.* 2007). These additional coordinate shifts depend both on the antenna model and on the latitude of the station. To account for these antenna-induced shifts, latitude-dependent functions have been published (Rebischung *et al.*, 2012):

$$dx = a + b\,\varphi + c_2\cos(2\varphi) + s_2\sin(2\varphi) + c_4\cos(4\varphi) + s_4\sin(4\varphi) \quad (3)$$

where dx is either an East, North or Up shift in mm
ϕ is the station latitude in radians.

However, the latitude-dependent models have variable precisions depending on the antenna model and should be used carefully. Moreover, the estimation of satellite clock parameters directly depends on the adopted antenna calibration models. Thus, clock products produced using different antenna calibrations (e.g igs05.atx and igs08.atx) cannot be used consistently for the production of coordinate time-series using absolute positioning.

III. DATA ANALYSIS

A. *Data used*

Three HEPOS stations were used to perform the data analysis. These stations were chosen based on their different characteristics regarding geographic location, magnitude of velocities and intensity of seasonal variations; moreover, they were chosen in areas that are not affected by any one of a series of strong earthquakes that stroke Greece in the years after HEPOS installation (Gianniou and Stavropoulou, 2016). Figure 1 shows the locations of the three stations. All three stations are equipped with Trimble NetRS receivers and Zephyr Geodetic antennas with radomes and are situated on single-floor, bulky buildings. The antennas are mounted on steel masts of 10 cm in diameter offering enhanced stability. The local environment of each station ensures open sky view and minimal multipath.

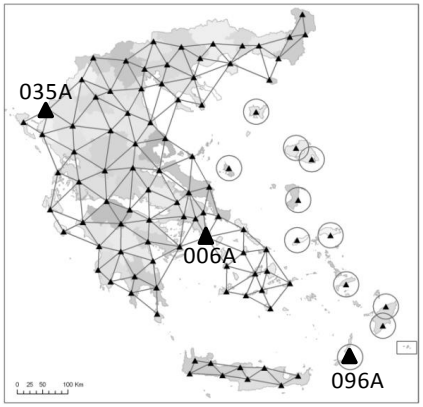

Figure 1. Locations of the stations used in this study

B. *PPP Processing*

The processing of the GPS data was performed with the Precise Point Positioning technique in static mode using the CSRS (Canadian Spatial Reference System) PPP software ver. 2.11.0. Coordinate time-series produced with this software can lead to velocities that agree to velocities obtained from relative positioning at sub-mm/yr level (Walpersdorf *et al.*, 2017; Gianniou

and Stavropoulou, 2016). Final precise orbits and clock parameters of the International GNNS Service (IGS) were used, the elevation mask was 7.5° and the processing interval was 15 sec, which is the sampling interval of the daily HEPOS RINEX files. For each station all available daily files from epoch 2008.0 to 2018.0 were processed.

C. *Coordinate time-series*

The PPP processing yielded coordinates expressed in different reference frames. Coordinate trans-formations were applied in order to express all solutions into a common reference frame. Following the methodology described in section II.B, IGS05 and IGS14 coordinates were transformed into IGb08, which was chosen as the common reference frame. Outliers were detected by visual inspection and excluded from further analysis. It is worth to mention that only a very small number of outliers were detected (2 for station 006A, 4 for 035A and 3 for 096A), which indicates the good quality of the raw data and the good performance of the PPP engine.

Figures 2 and 3 depict the time-series of Y coordinate for stations 096A and 035A, respectively. Clearly, there is a strong difference between the two stations regarding the stochastics of their time-series. In contrast to station 096A, station 035A is characterized by considerable seasonal variations. To investigate the seasonal variations separately for the horizontal coordinates and the heights, we further produced time-series for the horizontal coordinates (east, north) in the local system. These time-series are shown in Figures 16-19 in the Appendix. The seasonal variations become more obvious in Figures 4 and 5 that show the time-series of the height for stations 096A and 035A.

Seasonal signals are common in GPS time-series and may have various origins like pole tide effects, ocean tide loading, atmospheric loading, non tidal oceanic mass, groundwater loading, thermal expansion of bedrock as well as limitations in atmospheric and orbit models (Dong *et al.*, 2002; Ostini 2012). Depending on their origin, seasonal variations have different periods. For the time-series of Figures 3 and 5 the dominating periodic signal is clearly an annual variation. Examination of the power spectra of the time-series

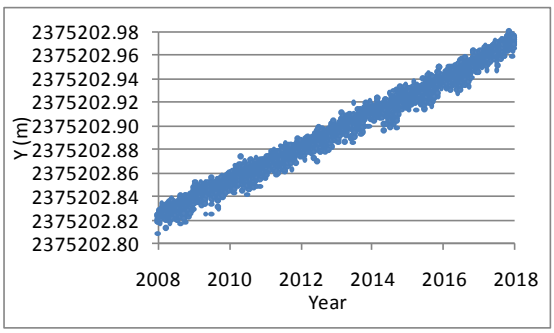

Figure 2. Time-series of Y for station 096A

for station 035A revealed also a semi-annual signal, but of much lower power. Aliased periodic signals, like the ones originating from M2 and O1 tidal components (Penna and Stewart, 2003) were not detected.

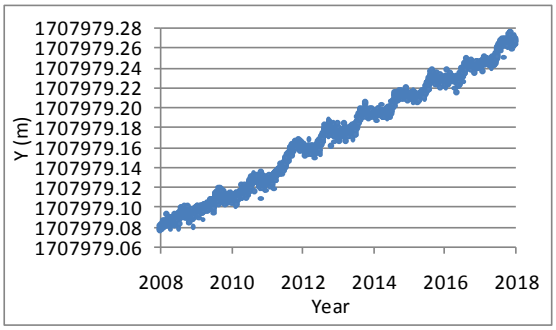

Figure 3. Time-series of Y for station 035A

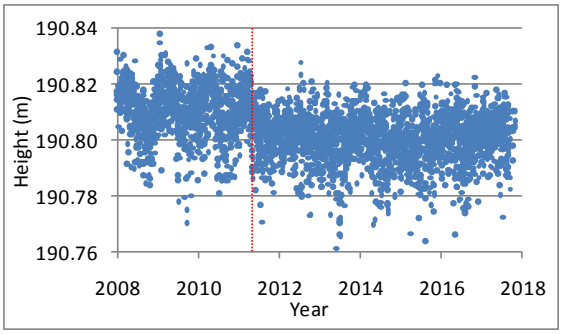

Figure 4. Time-series of height for station 096A

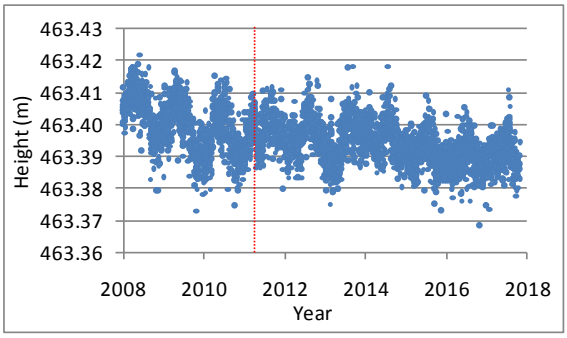

Figure 5. Time-series of height for station 035A

In Figures 4 and 5 the vertical dashed lines at epoch 2011.3 denote the transition from IGS05 to IGS08 (see Table 1). Looking at the time-series of Figure 4, a clear shift is obvious which correlates strongly with the epoch of the transition from IGS05 to IGS08. Such clear shifts could not be detected in the time-series of East and North coordinates. Nevertheless, in order to avoid undetected small shifts in the coordinate time-series and to ensure unbiased assessment of the role of the time-series' length in the velocity estimation, we considered in our data analysis the PPP coordinates obtained in IGS08 and IGb08, i.e. from epoch 2011.293 to epoch 2017.077.

D. *Velocities' estimation: role of time-series' length*

The velocities were estimated using linear regression. For the purpose of validating our results,

we compared the horizontal velocities obtained for station 006A with velocities that have been estimated for the same station in another study following a different methodology (relative positioning using GAMIT software; Chousianitis *et al.*, 2013). The comparison showed that the two solutions agree at the level of 0.2-0.3 mm/yr. Since the afore-mentioned study did not contain vertical velocities, it was not possible to make the same validation for the vertical velocities. As the estimation of vertical velocities is much more demanding, we believe that this should be investigated in a dedicated research focusing on the vertical component.

In order to assess the role of the time-series' length in the velocity estimation, the velocities of each station were estimated considering variable time-series length and they were compared to the longest solution. The shortest time-series considered had a length of one year, in order to allow semi-annual and annual signals to complete full cycles. Starting with a data length of one year, velocities were estimated for longer datasets increasing the data length by one day until the maximum time span of the IGS08 and IGb08 solutions was reached. Besides the difference to the longest solution, the R^2 value was also examined to assess the goodness of fit for each time-series.

Figures 6, 7 and 8 depict the error (difference to the longest solution) in velocity estimation for East, North and height as a function of the time-series length. By inspecting these Figures the following observations can be made:

1. The weakest velocity estimation for E and N (highest error and biggest variation) is observed for station 035A. This can clearly be attributed to the significant seasonal variations that are obvious in the coordinate time-series of 035A. The station with the most stable velocity estimation is 096A, which is least affected by seasonal variations.
2. The errors of velocity estimation (for East and North) of station 035A show a constant yearly pattern with a local minimum in February and a local maximum in the middle of the year. However, it is noteworthy to mention that this semi-annual signal does not repeat itself in the second half of each year.
3. A three-year time-series' length proved to be sufficient for the E and N velocities to converge to the correct values at a level better than ±0.001 m/yr. The exact length of the time-series that yielded a velocity error less than 1mm/yr is given for each station in Table 2.
4. A three-year time-series' length showed to be sufficient for the vertical velocities to converge to the correct values at a level better than ±0.002 m/yr. However, the accuracy of vertical velocities needs to be further investigated, due to the known weaknesses in estimating heights using GPS.
5. Four- or five-year long time-series allow for horizontal velocity accuracies at the level of few tenths of mm/yr. Figure 9 shows the year-by-year improvement of the velocity estimation. It is worth to notice the dramatic improvement achieved by increasing the 3-year time span to four years, whereas the improvement from four years to five years is considerably smaller.

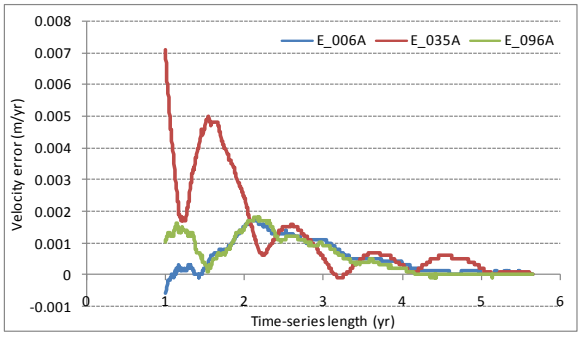

Figure 6. Error of velocity estimation (East)

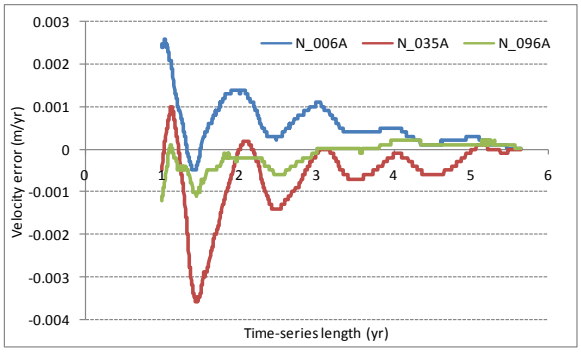

Figure 7. Error of velocity estimation (North)

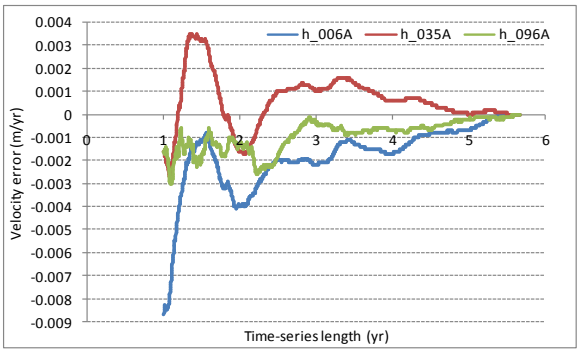

Figure 8. Error of velocity estimation (height)

Table 2. Required time-series length (in years) to ensure velocity error less than 0.001 m/yr

Station	time-series length (yr)		
	East	North	Height
006A	3.0	3.1	4.3
035A	2.9	2.7	3.7
096A	2.9	1.5	2.6

Generally speaking, the vertical component of the ITRF velocities is considerably smaller (at least by an order of magnitude) than the horizontal velocities. For the stations analyzed in this work the horizontal

velocities range between 0.011 and 0.023 m/yr while the height velocities are in the 0.001 m/yr level. Due to the increased noise level in the GPS height solutions, the estimation of velocities at the 1 mm/yr level becomes demanding. In order to shed more light on the accuracy of the estimated velocities, the R^2 values of the linear regression were examined. Figures 10, 11 and 12 show the R^2 value in dependence on the time-series length. Table 3 gives the R^2 values for the three-year long time-series. The uncertainty of estimating the height velocities is clearly reflected in the small R^2 values.

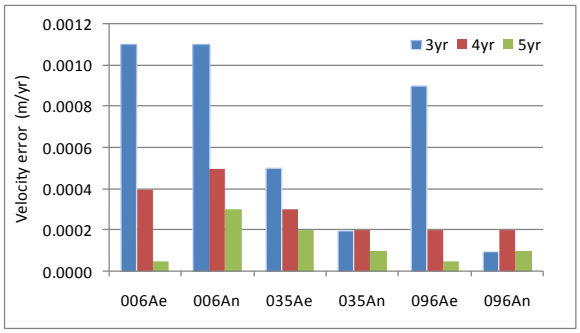

Figure 9. Error of velocity estimation for different time-series length (3, 4 and 5 years).

Table 3. R^2 values for three-year long time-series

Station	R^2 of linear regression		
	East	North	Height
006A	0.88	0.94	0.18
035A	0.94	0.86	0.01
096A	0.92	0.98	0.01

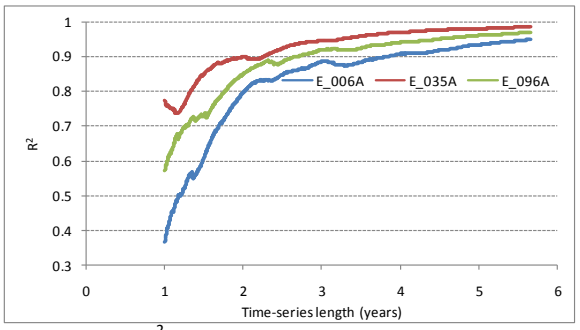

Figure 10. R^2 values of velocity estimation (East)

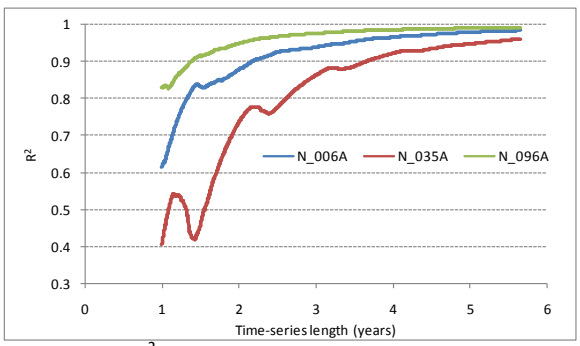

Figure 11. R^2 values of velocity estimation (North)

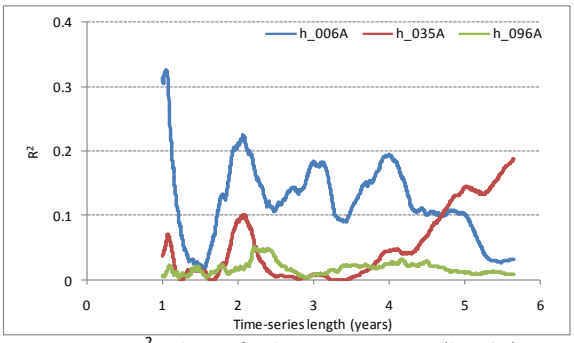

Figure 12. R^2 values of velocity estimation (height)

E. *Velocities' estimation: role of sampling interval*

The data analyzed above showed that five years of daily observations can lead to horizontal velocity estimation accurate to 0.1-0.3 mm/yr. In order to investigate if such accuracies require daily observations, or if it is possible to obtain comparable results using time-series of longer sampling interval, further analysis was carried out. More precisely, the velocities of each station were estimated using five different sampling intervals, i.e. 1, 7, 10, 15 and 30 days. The obtained results for velocity components of station 006A are shown in Figures 13-15 and in Figures 20-25 in the Appendix for stations 035A and 096A. Table 4 gives the E and N velocity errors (divergences from the daily solutions) for all tested sampling intervals. It can be seen that for data length 4 or 5 years, sampling intervals of 7, 10 and 15 days can yield velocities that coincide to the daily solutions at the level of 0.2 mm/yr.

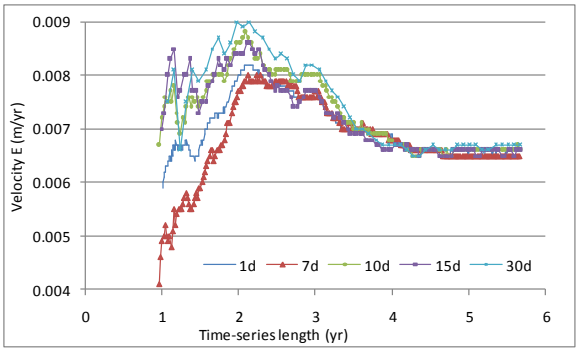

Figure 13. Velocity (East) for station 006A

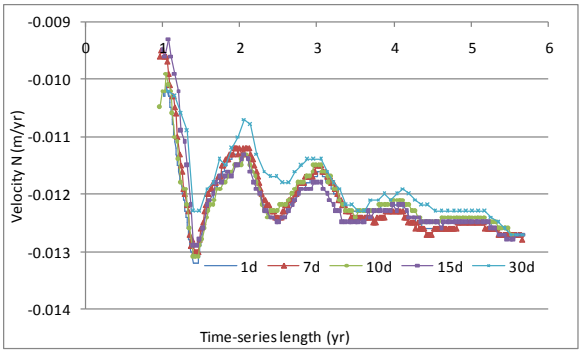

Figure 14. Velocity (North) for station 006A

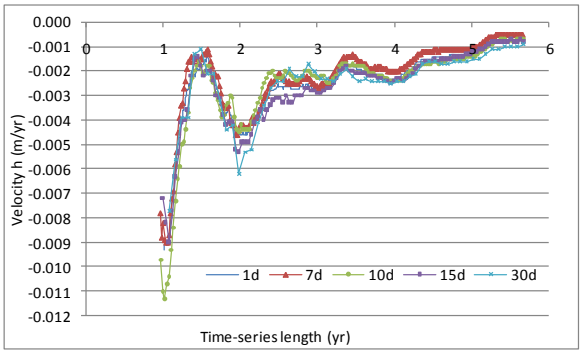

Figure 15. Velocity (height) for station 006A

Table 4. Velocity error (divergences from the daily solutions) for different sampling intervals and different time-series length (in m/yr) (maximum error for E and N velocities among all stations)

Length	Sampling interval			
	7 days	10 days	15 days	30 days
3 yr	0.0005	0.0006	0.0004	0.0004
4 yr	0.0001	0.0002	0.0001	0.0005
5 yr	0.0001	0.0001	0.0001	0.0002

IV. CONCLUSIONS

Based on the above described data analysis the following conclusions can be drawn regarding the velocity estimation from the PPP time-series:

1. Three years of daily observations can provide horizontal velocity estimations accurate to 1 mm/yr. This conclusion is in agreement with the generally accepted rule stating than three years of GPS observations are needed for reliable velocity estimation. In the literature a minimum required time span of 2.5 years (Blewitt and Lavallée, 2002; Dach *et al*., 2015) or 3 years (Calais *et al*, 2006) is suggested for velocity estimations.
2. In order to obtain horizontal velocity estimations accurate to 0.2 mm/yr, 4-5 years of observations are needed.
3. The magnitude of seasonal signals may be quite different among stations of the same network.
4. Seasonal effects can significantly affect the velocity estimation, particularly when a non integer number of years is used (see Fig. 6-8). Similar remarks can be found in the literature (Dixon and Mao, 1997).
5. At stations 035A and 006A a semi-annual signal appears only in the first half of the year, a phenomenon that should be further investigated.
6. Sampling intervals of 7, 10 and 15 days can yield horizontal velocities that match to that of the daily solutions at the level of 0.2 mm/yr, provided that at least 4 years of data are available.

V. ACKNOWLEDGEMENTS

The authors are grateful to two anonymous reviewers for their valuable comments.

References

Blewitt, G. and D. Lavallée (2002). Effect of annual signals on geodetic velocity. *J. Geophys. Res.: Solid Earth*, 107(B7), ETG-9.

Calais, E., J. Y. Han, C. DeMets and J. M. Nocquet (2006). Deformation of the North American plate interior from a decade of continuous GPS measurements. *Journal of Geophysical Research: Solid Earth*, 111(B6).

Chousianitis, K., A. Ganas and M. Gianniou (2013). Kinematic interpretation of present-day crustal deformation in central Greece from continuous GPS measurements. Journal of Geodynamics, 71, 1-13.

Dach, R., S.Lutz, P. Walser and P. Fridez (2015). Bernese GNSS software version 5.2.Astronomical Institute, University of Bern, Bern, Switzerland.

Dixon, T., and A. Mao (1997). A GPS estimate of relative motion between North and South America, *Geophysical Res. Lett.*, 24, 535–538.

Dong, P., P. Fang, Y. Bock, M.K. Cheng, and S. Miyazaki (2002). Anatomy of apparent seasonal variations from GPS-derived site position time series *J. Geophys. Res.*, 107(B4).

Gianniou, M. and I. Stavropoulou (2016). Estimation of tectonic velocities using GPS Precise Point Positioning: The case of Hellenic RTK network HEPOS.EUREF 2016 Symposium, May 25-27 2016, San Sebastian, Spain.

Kouba J. and P. Héroux (2001). GPS precise point positioning using IGS orbit products. *GPS Solutions* Vol. 5 No 2, pp. 12-28.

Hollenstein, C. (20016). GPS deformation field and geodynamic implications for the Hellenic plate boundary region. Swiss Federal Institute of Technology Zurich, Diss. ETH. 16593.

Ostini, L. (2012). Analysis and quality assessment of GNSS-derived parameter time series. Geodätisch-geophysikalische Arbeiten in der Schweiz. PhD thesis, University of Bern.

Penna, N. T. and M. P. Stewart (2003). Aliased tidal signatures in continuous GPS height time series, *Geophys. Res. Lett.*, 30(23), 2184.

Rebischung, P., J. Griffiths, J.Ray et al. (2012) IGS08: the IGS realization of ITRF2008. *GPS Solutions*, Vol 16, Issue 4.

Schmid R., P. Steigenberger, G. Gendt, M. Ge and M. Rothacher (2007). Generation of a consistent absolute phase center correction model for GPS receiver and satellite antennas. *Journal of Geodesy* 81(12): 781–798.

Walpersdorf, A., L. Pinget, P.Vernant, C. Sue, ans A. Déprez (2017). Deformation pattern of the Western Alps from two decades of campaign and permanent GNSS measurements. In: *EGU General Assembly Conference Abstracts* (Vol. 19, p. 3046).

Zumberge, J. F., M. B. Heflin, D. C. Jefferson, M. M. Watkins and F. H. Webb (1997). Precise point positioning for the efficient and robust analysis of GPS data from large networks, *J. Geophys. Res.*, 102(B3), 5005–5017, doi:10.1029/96JB03860.

APPENDIX

In continuation to Figures 2-3, the Figures 16-19 in this Appendix depict the East and North time-series for stations 096A and 035A.

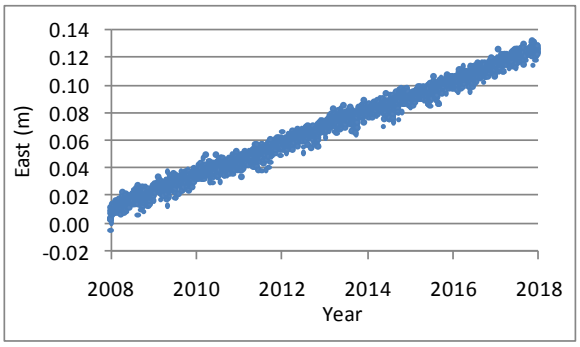

Figure 16. Time-series of East for station 096A

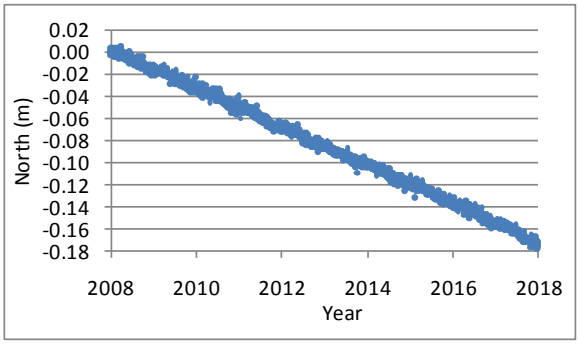

Figure 17. Time-series of North for station 096A

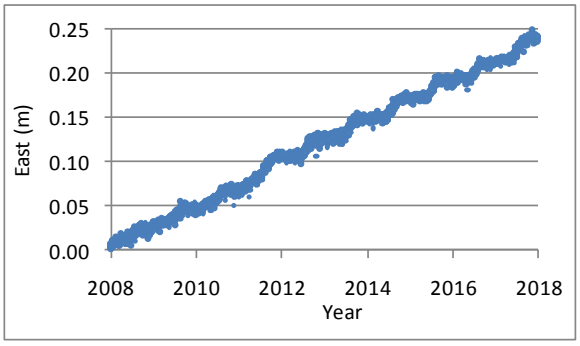

Figure 18. Time-series of East for station 035A

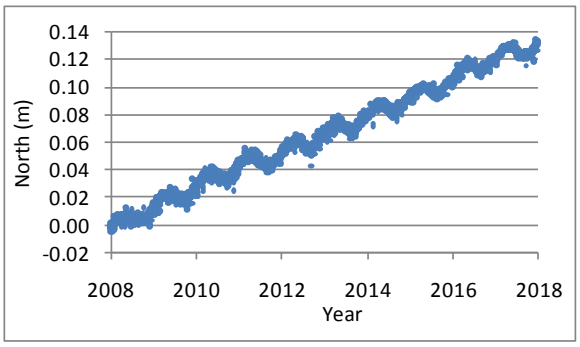

Figure 19. Time-series of North for station 035A

In continuation to Figures 13-15 the Figures 20-25 in the Appendix, give the velocity estimations for stations 035A and 096A for different sampling intervals.

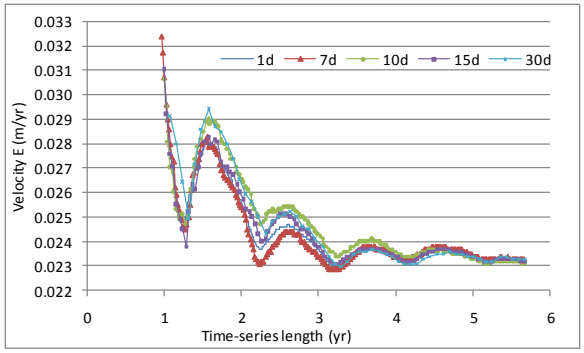

Figure 20. Velocity (East) for station 035A

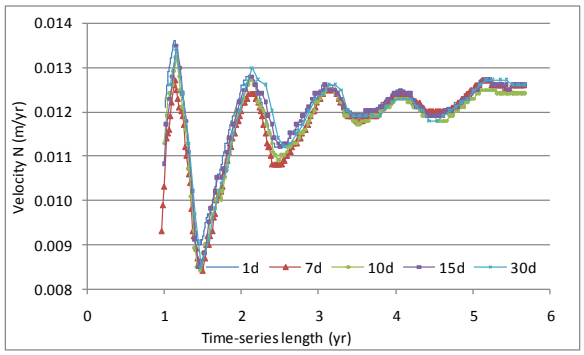

Figure 21. Velocity (North) for station 035A

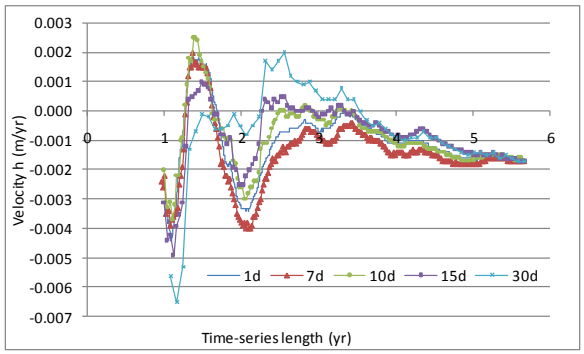

Figure 22. Velocity (height) for station 035A

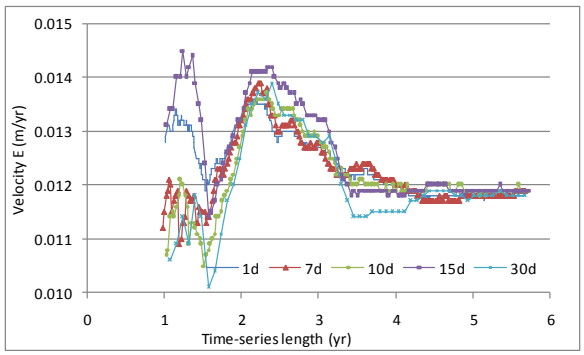

Figure 23. Velocity (East) for station 096A

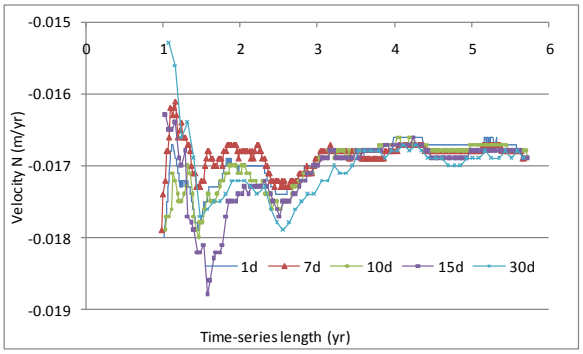

Figure 24. Velocity (North) for station 096A

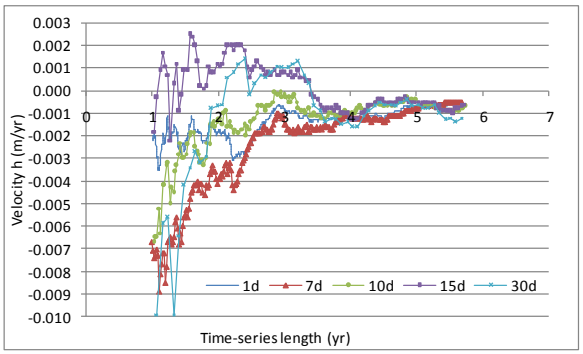

Figure 25. Velocity (height) for station 096A